

1 Detection of EEG dynamic complex patterns in disorders of
2 consciousness

3 **Running head:** EEG patterns in disorders of consciousness

4 Gabriel A. Della Bella MSc,^{1,2,†} Di Zang MD. PhD,^{3,4,5,6,7,8,†} Peng Gui PhD,^{9,†} Diego M. Mateos
5 PhD,^{10,11} Jacobo D. Sitt PhD,^{12,13} Tristan A. Bekinschtein PhD,¹⁴ Dragana Manasova PhD,^{12,15}
6 Benjamine Sarton MSc,^{16,17} Fabrice Ferre MSc,^{16,17} Stein Silva MD. PhD,^{16,17} Pedro W. Lamberti
7 PhD,^{2,18} Xuehai Wu MD. PhD,^{3,4,5,6,7} Ying Mao MD. PhD,^{3,4,5,6,7} Liping Wang PhD,^{9*} and Pablo
8 Barttfeld PhD,^{1*}

9 †These authors contributed equally to this work. *Co-senior authors.

10 1 Cognitive Science Group. Instituto de Investigaciones Psicológicas (IIPsi, CONICET-UNC), Facultad de
11 Psicología, Universidad Nacional de Córdoba, 5000, Córdoba, Argentina.

12 2 Facultad de Matemática Astronomía y Física (FaMAF), Universidad Nacional de Córdoba, 5000, Córdoba,
13 Argentina.

14 3 Department of Neurosurgery, Huashan Hospital, Shanghai Medical College, Fudan University, 200040,
15 Shanghai, China.

16 4 National Center for Neurological Disorders, 200040, Shanghai, China.

17 5 Shanghai Key Laboratory of Brain Function and Restoration and Neural Regeneration, 200040, Shanghai,
18 China.

19 6 Neurosurgical Institute of Fudan University, 200040, Shanghai, China.

20 7 Shanghai Clinical Medical Center of Neurosurgery, 200040, Shanghai, China.

21 8 Department of Neurosurgery, China-Japan Friendship Hospital, Beijing, 100029, China

22 9 Institute of Neuroscience, Key Laboratory of Brain Cognition and Brain-Inspired Intelligence Technology,
23 CAS Center for Excellence in Brain Science and Intelligence Technology, Chinese Academy of Sciences,
24 Shanghai 200031, China.

25 10 Consejo Nacional de Investigaciones Científicas y Técnicas (CONICET), Buenos Aires, Argentina.

26 11 Achucarro Basque Center For Neuroscience. Leioa, Vizcaya, Spain.

27 12 Sorbonne Université, Institut du Cerveau–Paris Brain Institute–ICM, Inserm, CNRS, APHP, Hôpital de la
28 Pitié Salpêtrière, 75013, Paris, France.

29 13 Inserm U 1127, F-75013 Paris, France.

30 14 Department of Psychology, University of Cambridge, Cambridge, CB2 3EB, United Kingdom.

31 15 Université Paris Cité, 75006 Paris, France.

32 16 Réanimation URM CHU Purpan, Cedex 31300 Toulouse, France.

33 17 Toulouse NeuroImaging Center INSERM1214, Cedex 31300 Toulouse, France.

34 18 Institute of Theoretical Physics, Jagiellonian University, ul. Łojasiewicza 11, 30–348 Kraków, Poland.

35

36 **The corresponding author contact information:**

37 Peng Gui. Institute of Neuroscience, Key Laboratory of Primate Neurobiology, CAS Center for Excellence in
38 Brain Science and Intelligence Technology, Chinese Academy of Sciences, Shanghai 200031, China.
39 pgui@ion.ac.cn

40 **Abstract**

41 A major challenge in cognitive neuroscience is developing reliable diagnostic tools for
42 Disorders of Consciousness (DoC). Detecting dynamic brain connectivity configurations
43 holds great promise for advancing diagnostics. Evidence indicates that certain fMRI-
44 derived connectivity patterns are closely tied to the level of consciousness. However, their
45 clinical utility remains constrained by practical limitations. In this study, we introduce EEG-
46 based brain states as a real-time, bedside tool for detecting periods of enhanced brain
47 activity in DoC patients. We analyzed data from 237 patients with chronic and acute DoC
48 from three different centers and identified five EEG functional connectivity recurrent brain
49 patterns. The occurrence probabilities of these patterns were strongly correlated with
50 patients' levels of consciousness. High-entropy patterns were found exclusively in healthy
51 participants, while low-entropy patterns became more prevalent with increasing DoC
52 severity, crucially predicting individual recovery outcomes. To assess the real-time
53 applicability of this approach, we conducted tests demonstrating reliable, real-time
54 estimation of patient brain patterns, confirming the feasibility of bedside detection. Our
55 findings highlight the potential of EEG for real-time, bedside monitoring of brain dynamical
56 connectivity patterns, significantly deepening our understanding of the neural dynamics
57 underlying consciousness and paving the way for future discoveries in brain state
58 research.

59

60

61

62

63

64

65

66

67

68 **Introduction**

69 Diagnosing disorders of consciousness (DoC) and prognosing patients' evolution remain
70 a major medical challenge. Current classifications of DoC are based primarily on clinical
71 evaluations of arousal and awareness, leading to the categorization of patients into a
72 heterogeneous set of categories with definitions that are still evolving^{1,2}. However, these
73 assessments, which rely on overt behavioral responses, are inherently limited and are
74 susceptible to bias from factors affecting motor output (e.g. locked-in syndrome)^{3,4} or
75 language function (e.g. aphasia)^{5,6}. As a result, diagnostic errors are common, with
76 misdiagnosis rates estimated as high as 40%⁷, often leading to critical treatment decisions.

77 Given these limitations, there is a growing need for objective, neurophysiological markers
78 that can provide a more accurate assessment of consciousness. One promising avenue
79 of research lies in the study of brain signal complexity and information dynamics. In this
80 context, entropy, a measure of the unpredictability or disorder within a system, has
81 emerged as a powerful tool to characterize different states of consciousness, with
82 theoretical and practical implications. Studies in neuroscience have extensively explored
83 the relationship between entropy and consciousness, particularly in the contexts of coma,
84 anesthesia, and sleep⁸⁻¹⁰. Higher entropy has been associated with wakefulness and
85 cognitive flexibility, whereas lower entropy reflects diminished neural complexity, often
86 observed in unconscious states^{11,12}. Recent findings indicate that brain entropy
87 systematically decreases in coma, anesthesia, and deep sleep, reflecting a shift toward
88 more predictable and less integrated neural states^{8,13}. This pattern is consistent with the
89 loss of long-range functional connectivity and thalamocortical disruptions observed in
90 unconscious states¹⁴. A set of studies have proposed that consciousness emerges from
91 the brain's dynamic organization, following the MaxCon (Maximization of Configurations)
92 principle¹⁵⁻¹⁷. This framework suggests that conscious states arise when the brain
93 optimally balances integration and segregation of information, maximizing network
94 complexity. By analyzing entropy and brain connectivity across different states (e.g.,
95 anesthesia, coma, wakefulness), the authors provide evidence that consciousness
96 corresponds to maximal configurational diversity and information distribution.

97 However, entropy-based approaches alone may not fully capture the complexity of
98 conscious states. Sanz Perl et al.¹⁸ demonstrated that macroscopic brain activity deviates
99 from equilibrium during wakefulness, a property that is lost in unconscious states. Using
100 entropy production and the curl of probability flux in phase space, they showed that
101 wakefulness is characterized by persistent non-equilibrium dynamics, whereas
102 unconscious states, including those induced by propofol and ketamine anesthesia, shift
103 toward equilibrium conditions. In active states such as wakefulness, the number of
104 possible system configurations, representing the different ways in which brain regions can
105 connect, is maximized. From the standpoint of statistical physics, this corresponds to a
106 tendency to maximize entropy. In contrast, altered states such as sleep¹⁹, anaesthesia²⁰,
107 or DoC²¹ show a reduction in the number of possible configurations, leading to lower
108 entropy¹⁶. This perspective aligns with the idea that a rich repertoire of network
109 configurations, rather than just a high level of entropy, is essential for conscious
110 experience. Beyond traditional measures of neural complexity, recent work has framed
111 consciousness as a non-equilibrium phenomenon, highlighting the brain's deviation from
112 thermodynamic equilibrium as a fundamental signature of awareness¹⁸. Various theories
113 of consciousness have incorporated entropy as a fundamental principle to explain
114 conscious states and their fluctuations. In general, these theories suggest that
115 consciousness emerges from neural dynamics that balance order and disorder, where
116 entropy reflects the brain's ability to process information flexibly and adaptively. From a
117 thermodynamic perspective, the theory of the brain as a non-equilibrium system posits
118 that consciousness arises when the brain operates far from thermodynamic equilibrium,
119 maintaining a stable yet highly variable dynamic^{18,22}. According to this view, unconscious
120 states reflect a reduction in neural complexity and a shift toward more predictable,
121 equilibrium-like dynamics. Signal entropy has been widely studied as a correlate of
122 consciousness, with measures derived from EEG time-series (e.g., spectral entropy,
123 Lempel-Ziv complexity) consistently showing reduced complexity in unconscious states.
124 However, these approaches primarily capture local neural signal variability rather than
125 large-scale network coordination. In contrast, connectivity entropy quantifies the diversity
126 of functional interactions across brain regions, offering a complementary perspective on
127 the neural dynamics of consciousness. Together, these theories suggest that
128 consciousness is deeply linked to the regulation of entropy in the brain. While conscious
129 states are characterized by high but structured entropy, unconscious states reflect a

130 decline in complexity and a shift toward equilibrium-like dynamics. Understanding how
131 entropy interacts with other neural properties remains a key challenge in consciousness
132 research.

133

134 Recent advancements in neuroimaging, guided by the aforementioned findings on entropy
135 and complexity, as well as connectionist theories of consciousness^{8,23–26}, have sought to
136 characterize conscious states by identifying brain activity patterns that may not be
137 detectable through behavioral assessments. These techniques have emerged using
138 active cognitive tasks^{21,27–29}, spontaneous brain activity^{9,30–32}, and external stimulation
139 paired with EEG responses^{33–35}, providing clinicians with new tools to detect
140 consciousness. Among these methods, one of the most promising approaches is based
141 on studying signatures of consciousness through the detection of fMRI-based “brain
142 states”^{13,36–39}, which is especially well suited to detect spontaneous, transient shifts in
143 brain activity. These brain states refer to recurring patterns of functional connectivity
144 obtained through unsupervised clustering of dynamical connectivity matrices that can
145 reveal these shifts (typically lasting from 5 to 60 seconds³⁶). Research indicates that the
146 properties of the brain states are strongly modulated by levels of arousal and
147 consciousness. In awake humans and monkeys a diverse range of brain states exists,
148 including those with high connectivity, high entropy, and negative correlations^{13,36,38,39}.
149 Conversely, in cases of DoC or under sedation, there are significant changes in the
150 observed brain states: the richer variety of brain states diminishes, and only low-
151 connectivity, low-entropy states —shaped by the underlying structural connectivity—
152 persist^{9,37}. These findings are in line with dynamical systems simulations^{40,41} showing that,
153 for low coupling strength between brain areas —a configuration resembling DOC
154 condition—spontaneous neuronal activity remains but it is restricted to a single stable
155 connectivity pattern, defined by the fixed network of structural connectivity. As connectivity
156 between brain regions increases, the system undergoes a transition to multistability,
157 allowing for a diverse set of possible patterns. This transition is considered crucial for
158 sustaining conscious states.

159 However, the reliance on fMRI for detecting brain states presents significant practical
160 challenges in the clinical management of DoC. Transporting patients with life-supporting
161 devices to MRI scanners is often unfeasible, and repeated scanning over long periods is
162 required to capture the transient periods of heightened brain activity, which is impractical

163 in a scanner setting. In contrast, EEG offers a more accessible and real-time alternative,
164 allowing bedside assessments that could provide critical insights into patients' residual
165 brain function and consciousness. By leveraging EEG-based brain state detection, we can
166 move toward more personalized patient care, allowing clinicians to monitor transient
167 changes in brain dynamics.

168 In this study, we analyzed one of the largest cohorts of DoC patients to date, comprising
169 237 patients and 101 healthy controls from three independent clinical centers, aiming to
170 bring EEG-based consciousness detection closer to clinical application. We expanded
171 upon previous work that focused mainly on chronic DoC, such as Unresponsive
172 Wakefulness Syndrome (UWS) and Minimally Conscious State (MCS), by including both
173 chronic and acute patients. The acute group included comatose individuals with low
174 Glasgow Coma Scale (GCS) scores, with an average of 14 days since brain injury. Our
175 goal was to identify EEG-based brain states and explore their diagnostic and prognostic
176 potential across the full spectrum of DoC. (Fig. 1A). Our findings revealed and
177 characterized five distinct EEG functional connectivity brain states, whose occurrence
178 probability was closely associated with the level of consciousness. High-entropy brain
179 states were predominantly observed in conscious subjects, while low-entropy states
180 became more probable with increasing DoC severity. Moreover, we found that transient
181 patterns of high-entropy connectivity — akin to those seen in healthy individuals — could
182 occasionally be detected in DoC patients. The occurrence probability of these patterns
183 provided valuable diagnostic information and offered predictive insights into patient
184 outcomes. Finally, we demonstrated that these transient states of enhanced connectivity
185 could be detected in real-time using bedside EEG, highlighting the feasibility of this
186 method for continuous patient monitoring and neuroprognostication (Fig. 1).

187 **Results**

188 **Methodological overview**

189 The analyses applied in this work are illustrated in Fig. 1. EEG data from three distinct
190 sites were first transformed into symbolic representations using weighted Symbolic Mutual
191 Information (wSMI)²¹ (see Supplementary Methods and Fig. S1 for a full description of the
192 process). This measure identifies non-random joint fluctuations between two EEG signals,
193 allowing for the detection of meaningful patterns in brain connectivity. Next, k-means
194 clustering was employed on these wSMI connectivity matrices to identify recurring
195 connectivity patterns across all subjects, referred to as “brain states”^{13,37,38} (Fig. 1A). These

196 brain states were then sorted based on the Shannon entropy of the distribution of
197 connectivity values. Each brain state was classified by its proximity to the connectivity
198 matrices, resulting in a probability distribution for each subject (Fig. 1A, right). To
199 summarize the properties of these brain states, we calculated the Weighted Entropy (WE),
200 which represents the average entropy weighted by the probabilities. The WE metric
201 reflects the diversity and complexity of connectivity patterns across brain states, with
202 higher WE values indicating more varied and complex connectivity. To investigate the
203 relationship between these brain states and clinical outcomes, patients were categorized
204 into three groups based on their clinical evolution: *improvement* (e.g., transition from UWS
205 to MCS), *no change* (e.g., staying in the same condition), and *deterioration* (e.g., transition
206 from MCS to UWS).

207 **Detection of EEG brain states**

208 We identified five distinct EEG brain states, with the value of five determined using the
209 Elbow method⁴² (Fig. S2; see Supplementary Material for details), each characterized by
210 unique connectivity patterns. To streamline analysis and comparison, we ranked the brain
211 states by entropy levels (Fig. 2A), assigning numbers in descending order. Consistent with
212 previous findings in fMRI studies, brain states 1 and 2 displayed the highest entropy and
213 complexity (Fig. 2D). These states displayed a broad spectrum of connectivity values,
214 ranging from weak to strong connections across electrodes in a topographical map,
215 suggesting the presence of connectivity hubs in parietal regions (Fig. 2A). On the opposite
216 end of the entropy scale, brain states 4 and 5 exhibited a completely different connectivity
217 pattern. These states showed a narrow connectivity range with uniformly low connectivity
218 values, leading to a homogeneous distribution of connections across the scalp (Fig. 2A,
219 right). Using hierarchical decomposition analysis of the brain state space, we observed
220 similarities according to the Manhattan distance and positions between the different brain
221 states (Fig. 2C). Brain states 4 and 5 formed a cluster with the highest similarity, followed
222 by their merging with brain states 3 and 2 (Fig. 2C). Brain state 1 exhibited the greatest
223 distance from the other brain states, indicating its distinctiveness in the multidimensional
224 space.

225 **EEG brain states rates of occurrence across levels of consciousness**

226 Figure 2B depicts the distribution of brain states across different groups based on the
227 severity of DoC. Both the probability of each brain state (Fig. 2B) and the average WE
228 (Fig. 2E) were consistently modulated by the participant's condition. Compared to controls,

229 the patients' probability of high-entropy brain states diminished (Fig. 2B), the probability
230 of low-entropy states increased, and the average weighted entropy decreased (Fig. 2E).
231 As DoC severity increased from MCS to UWS to Acute, the WE progressively shifted
232 towards lower values in patients compared to controls (Fig. 2E) ($F_{3, 153.1} = 25.45$, $p =$
233 2×10^{-13}). Significant differences in WE were observed between the control group and all
234 patient groups (Healthy vs. MCS [-0.01141 ± 0.00254], $t\text{-ratio}(294.8) = -4.497$, $p =$
235 0.0001], Healthy vs. UWS [-0.01521 ± 0.00250], $t\text{-ratio}(294.9) = -6.081$, $p < 0.0001$],
236 Healthy vs. Acute [-0.02627 ± 0.00440], $t\text{-ratio}(82.1) = -5.967$, $p < 0.0001$]). However,
237 within the patient group, significant differences in WE were found only between MCS and
238 Acute ($[-0.01486 \pm 0.00515]$, $t\text{-ratio}(54.1) = -2.883$, $p = 0.028$]).

239 To ensure the robustness of our findings, we conducted separate analyses for each
240 center, confirming that the observed patterns held across all datasets (Fig. S3A and
241 Supplementary Methods). To further validate our results, we performed a cross-validation
242 approach, using centroids calculated in one center and testing them in another, which
243 confirmed the generalizability of our findings (Fig. S3 B, C). Additionally, these findings
244 remained stable even when reducing the number of EEG channels, as analyses with 64
245 and 32 channels yielded similar results to those obtained with 128 channels (Fig. S4). This
246 consistency across datasets, channel configurations, and validation methods strengthens
247 the reliability of our results.

248 **Patient-Specific EEG Brain States**

249 To refine our analysis, we re-ran the clustering algorithm, this time excluding data from
250 healthy controls. This approach allowed us to focus exclusively on the portion of the
251 multidimensional space occupied by the patient's data, enabling a more detailed
252 characterization of their EEG brain specific to the patients. To differentiate these newly
253 identified states from those obtained in the full dataset, we refer to them as Patient-Specific
254 Brain States (PBS), labeled as PBS1, PBS2, and so on. For this analysis, we combined
255 data from the Paris and Shanghai datasets while excluding the Toulouse dataset to avoid
256 collinearity issues, as the Toulouse dataset contained only acute patients. By restricting
257 the analysis to the Paris and Shanghai datasets, we were able to perform a mixed model
258 analysis on chronic patients and evaluate the method's potential for both prognosis and
259 diagnosis.

260 As expected, the newly identified brain states exhibited significantly lower wSMI values
261 and more diffuse topographies (Fig. 3A) and lower levels of LZ complexity and entropy
262 (Fig. 3C). Consistent with our previous findings, the probability of each individual brain
263 state (Fig. 3B), and WE (Fig. 3D) varied across patient groups, indicating that as the
264 severity of DoC increased from MCS to UWS, WE progressively shifted towards lower
265 values (Fig. 3D) ($F_{3, 183.82} = 18.7$, $p = 1.2 \times 10^{-10}$). Using centroids obtained exclusively from
266 patient data, we observed significant differences between MCS and UWS (95% CI
267 [0.00344, 0.00728], $t\text{-ratio}(332.1) = 2.793$, $p = 0.0282$).

268 **Prognostic Value of EEG Brain States**

269 Next, we investigated the potential of our methodology in predicting patient prognosis. In
270 chronic patients, we found a significant relationship between patient outcomes and WE
271 ($F_{2, 178.6} = 4.808$, $p = 0.009$; Fig. 4A and Fig. S5). Specifically, patients who showed
272 improvement in their condition (i.e., transitioning from UWS to MCS) had higher WE
273 (including patients who transitioned from MCS to MCS+ in the improvement group did not
274 change the results; however, we excluded them from the analysis as they represented
275 only three cases), while those who experienced deterioration (transitioning from MCS to
276 UWS or dying) had lower WE. Pairwise comparisons adjusted for multiple comparisons
277 revealed significant differences between the Deteriorate and Improve groups (95% CI
278 [0.000759, 0.00740] $p = 0.0115$). However, no significant differences were observed
279 between the Deteriorate and No change groups (95% CI [-0.00245, 0.00448], $p = 0.77$) or
280 the No change and Improve groups (95% CI [-0.000156, 0.00628], $p = 0.065$).

281 Similarly, in acute patients we found a significant relationship between patient outcomes
282 and WE ($F_{2, 38} = 5.947$, $p = 0.00566$; Fig. 4B). Significant differences were observed
283 between the No change group (patients transitioning to UWS) and the Deceased group
284 (0.0521, 95% CI [0.0085, 0.0958], $p = 0.016$), as well as between the Improve group
285 (patients transitioning to MCS) and the Deceased group (0.0522, 95% CI [0.0121, 0.0922],
286 $p = 0.008$). However, no significant differences were found between the Improve and No
287 change groups (5×10^{-5} , 95% CI [-0.039, 0.039], $p = 0.99$).

288 **Towards Real-Time EEG Monitoring of Patients**

289 To assess the practical potential of this methodology, its performance was tested in a
290 simulated real-time bedside setting. Although real-time data were not available, we

291 conducted a simulation of real-time assessment on acute patients using our pipeline (see
292 Supplementary Methods for a detailed explanation of the procedure). We classified
293 segments of raw EEG signals into one of the five brain states previously defined for the
294 patients (Fig. 1B). We compared the similarity between offline and real-time brain state
295 distributions in patients, along with their corresponding WE values. Statistical analysis
296 revealed no significant differences in WE values between the two conditions ($F_{1,78} = 0.713$,
297 $p = 0.401$), indicating that the real-time classification effectively replicated the distribution
298 observed in the offline analysis (Fig. 5A). Figure S5B displays the high degree of similarity
299 between offline and real-time classifications. The average WE values for each patient
300 remained highly stable between the two conditions ($R = 0.98$) (Fig. 5B), suggesting that
301 our methodology can reliably capture patient-specific brain states in a real-time context.
302 We also quantified the similarity between real-time and offline distributions using a
303 bootstrap method (see Supplementary Methods for details). To assess this similarity, we
304 computed the Jensen-Shannon divergence between the distributions (Fig. 5C). The
305 results showed that the divergence between real-time and offline distributions was not
306 significantly different from random fluctuations when classifying real-time data based on
307 the offline brain states of the same acute patients ($p = 0.47$).

308 We further explored the potential of our simulated real-time method by assessing its ability
309 to predict prognosis, as we previously did in the offline analysis. In acute patients, we
310 found that real-time mean values, obtained from a single real-time recording, could
311 distinguish between patients who improved and those who deteriorated just as effectively
312 as the offline analysis ($F_{2,38} = 7.47$, $p = 0.001$). We found significant differences in No
313 change vs. Deteriorate (0.05, 95% CI [0.01, 0.09], $p = 0.004$) and Improve vs. Deteriorate
314 (0.05, 95% CI [0.01, 0.08], $p = 0.003$) but no significant difference between in No change
315 vs. Improve (-0.002, CI [-0.03, 0.03], $p = 0.97$). Next, we used the probability values of
316 each brain state as features to train a Logistic Regression classifier to differentiate
317 between the control and acute groups. The model, evaluated using a leave-one-out cross-
318 validation approach, achieved an AUC of 0.80, an accuracy of 0.76, and an F1-score of
319 0.81. These results demonstrate that the real-time classification framework effectively
320 captures meaningful differences between conditions, highlighting its potential for practical
321 application.

322 **Discussion**

323 In this study, we investigated EEG brain states in healthy individuals and patients with
324 DoC, identifying distinct brain states and demonstrating their relevance to patient
325 categories and recovery probabilities. We also established the feasibility of real-time,
326 bedside brain state detection, offering a reliable estimation of the patient's current brain
327 state.

328 **EEG Brain States and Their Link to Consciousness**

329 Our findings align with previous research on functional connectivity in DoC patients, as
330 the EEG brain states we identified reflect topographical patterns consistent with those
331 seen in prior research on wakefulness and DoC states^{13,36,37}. Specifically, brain states 1
332 and 2 exhibit striking similarities with the topographies from healthy individuals in time-
333 averaged wSMI estimations^{28,29}. These topographies indicate a temporal organization
334 characterized by long-range coupling between brain regions, resulting in distinct functional
335 connectivity patterns. Notably, these patterns encompass both low and high magnitude
336 wSMI values and feature a prominent connectivity hub located at bilateral parietal cortices.
337 Conversely, brain states 4 and 5 resemble those observed in fMRI studies conducted on
338 anesthetized monkeys^{39,43} and DoC patients¹³ using both EEG and fMRI modalities. These
339 patterns are featured by highly distributed and homogeneous low connectivity with
340 diminished or very weak correlation or mutual information.

341 These results reinforce theories of consciousness emphasizing long-distance connectivity
342 and dynamic interaction between brain regions as critical for the emergence and
343 maintenance of conscious states^{24,26}. According to current models of consciousness, rich
344 and dynamic functional interactions, along with a diverse repertoire of connectivity
345 patterns, are considered key aspects of conscious processing. These dynamics rely on a
346 certain level of coupling between brain regions, enabling the integration of segregated
347 neural processes and supporting potential conscious awareness^{34,44,45}. Conversely, in
348 conditions such as anesthesia, DoC, or non-rapid eye movement (NREM) sleep, brain
349 regions exhibit decreased coupling and functional connectivity converges into a low
350 connectivity pattern that aligns with the underlying anatomical connections. This state is
351 characterized by spatially homogeneous and weak connectivity, with limited segregation
352 or integration of neural activity. It represents a stable and long-lasting brain state
353 associated with reduced conscious awareness^{38,43}.

354 **The Role of Entropy in Brain State Classification**

355 An essential consideration in entropy-based assessments of consciousness, such as our
356 approach, is that variability in connectivity, rather than the absolute strength of
357 connections, is the primary factor driving changes in entropy. Our analysis comparing
358 connectivity entropy with local signal entropy revealed that while both measures decrease
359 in unconscious states, local signal entropy showed limited classification power in our
360 dataset (Fig. S6), suggesting that large-scale functional network diversity is a stronger
361 marker of consciousness than local neural complexity alone. This distinction is crucial
362 when analyzing brain states such as epilepsy and coma. In epilepsy, for instance, neural
363 connections are abnormally strong and highly synchronized, yet this excessive rigidity
364 results in low entropy due to a lack of flexible state transitions. A similar pattern is observed
365 in coma, where patients predominantly remain in state 5, a highly stable neural
366 configuration with minimal variation over time. Despite having wSMI values that may
367 appear comparable to wakefulness in absolute terms, the key difference lies in the lack of
368 fluctuation in these values. This reflects the brain's failure to dynamically adapt and
369 process both internal and external information. Thus, entropy-based approaches should
370 not only consider connection strength but also the capacity of the system to transition
371 between different states, as this flexibility is likely a crucial feature of conscious
372 processing. Another crucial aspect to consider is the role of connection variability in
373 entropy, rather than just the strength of connectivity. Studies using wSMI and similar
374 metrics indicate that high entropy is associated with dynamic, flexible neural connections,
375 not necessarily stronger connections⁹. In conditions such as epilepsy, brain activity is
376 highly synchronized, with strong but rigid connections, leading to a low entropy state
377 despite intense neural activity. This suggests that entropy-based measures should
378 account for connection variability rather than absolute connectivity strength when
379 assessing consciousness. While WE is not a direct measure of complexity, it provides
380 insights into the variability of brain state organization, reflecting both the range of
381 connectivity values and the temporal changes in these patterns. This aligns with previous
382 studies that have used temporal dynamics to understand functional connectivity in the
383 brain^{8,46}.

384 **Clinical Applications and Real-Time Monitoring**

385 Using EEG brain states, we successfully differentiated healthy participants from patients
386 and discriminated between DoC categories. Moreover, we have shown that applicability
387 of our methods is not reliant on high-density EEG systems. While our approach does not

388 achieve exceptional classification scores compared to recent multimodal approaches that
389 combine multiple metrics, it offers unique advantages. One advantage of our approach is
390 the ability to detect specific windows of enhanced brain activity in real time. This could
391 improve the classification performance of multivariate models that currently do not account
392 for individual fluctuations over time. By combining current EEG classification methods with
393 the identification of these transient brain states, we may develop a powerful tool for the
394 diagnosis and prognosis of patients. Moreover, these tools could foster more productive
395 interactions between healthcare providers and patients by focusing on moments when the
396 patient exhibits brain states 1 and 2. Furthermore, our findings suggest that even the
397 presence of complex brain states can offer valuable insights into the DoC category and
398 patient outcomes. The real-time detection of EEG brain states presents a novel
399 opportunity for bedside diagnosis and intervention. Although richer brain states are rare in
400 DoC patients, traces of these states can still be identified across all DoC categories. This
401 suggests that patients' brains briefly visit richer connectivity patterns. Detecting these
402 transiently rich brain states could potentially be valuable for identifying windows of
403 momentarily enhanced cognition in patients, which can inform optimal communication and
404 intervention strategies. Interventions during these brief states of altered brain dynamics
405 may lead to sustained exploration of the brain state repertoire and possibly associated
406 behavioral changes. Similar approaches, such as deep brain stimulation, have shown
407 promising results in modulating fMRI brain states in anesthetized monkeys³⁹, suggesting
408 its potential applicability in DoC patients to drive the brain state towards cognitively rich
409 configurations.

410 **Limitations and Open Questions**

411 We were able to discriminate between different DoC subcategories only after excluding
412 healthy controls from the analysis, due to the variability introduced by healthy individuals.
413 The use of k-means clustering posed limitations, as it partitions data into equally sized
414 clusters, impacting the granularity of our findings. Future research should explore more
415 advanced clustering methods that can adjust cluster sizes dynamically to improve
416 discrimination between patient subcategories.

417 A significant methodological challenge in using EEG to study brain states is the lack of
418 direct information on specific brain regions, unlike fMRI. EEG signals cannot directly map
419 functional to structural connectivity, although structural connectivity plays a crucial role in

420 shaping brain states, especially under low vigilance. Our approach addressed this by
421 classifying brain states based on entropy. This allowed us to capture the dynamics of brain
422 states without needing direct structural data. Notably, our entropy-based sorting closely
423 mirrored the anatomical organization observed in fMRI studies, suggesting that EEG could
424 offer a reliable means of characterizing brain state dynamics. Future work should explore
425 how to model these results without relying on structural matrices, potentially developing
426 EEG-based models grounded in functional connectivity backbones.

427 A key limitation of this study, and of research on brain states in general, is the uncertainty
428 regarding their relationship to subjective experience. Neither our study nor previous works
429 have systematically examined whether the same brain state corresponds to similar
430 cognitive or perceptual experiences. While high-entropy states are predominantly
431 observed in conscious individuals, their occasional presence in DoC patients does not
432 necessarily imply awareness. Likewise, the frequent occurrence of low-entropy states in
433 healthy controls does not indicate unconsciousness during those periods. Understanding
434 the functional significance of these brain states requires further investigation into their
435 cognitive content, ideally incorporating experience sampling alongside neurophysiological
436 monitoring.

437 A particularly intriguing finding is the persistence of low entropy brain states such as
438 number 5 in healthy controls, which aligns with previous fMRI studies but remains poorly
439 understood. This state could reflect transient microsleep episodes, a common but often
440 overlooked phenomenon in resting-state paradigms. Alternatively, it may not indicate a
441 loss of consciousness but rather effortful information processing, occurring between
442 cognitively demanding tasks while subjects remain vigilant. Without direct experience
443 sampling, it is unclear whether this state corresponds to altered awareness. Future
444 research should aim to distinguish between these possibilities by combining EEG-based
445 connectivity analysis with subjective reports and objective wakefulness measures such as
446 eye-tracking or polysomnography.

447 More broadly, the classification of brain states is constrained by the assumption that they
448 represent discrete functional configurations with distinct cognitive correlates. One key
449 limitation is the lack of direct association between these states and specific mental
450 content. Neither our study nor previous works have systematically investigated whether
451 the same brain state corresponds to similar subjective experiences, leaving open the

452 possibility that distinct cognitive or perceptual states could map onto the same connectivity
453 configuration. Additionally, k-means clustering assumes that the identified states are
454 equally distributed and well-separated in the feature space. However, the robustness of
455 our clustering analysis regarding the number of brain states to identify (Fig. S2), and the
456 stability of brain states across resting-state and task conditions (Table S2), highlight both
457 strengths and challenges in defining brain states. On one hand, the consistency of results
458 across different clustering solutions and experimental conditions suggests that these
459 findings are not an artifact of arbitrary parameters. On the other hand, this same
460 robustness raises fundamental questions about what constitutes a "brain state"—if states
461 remain unchanged across cognitive conditions, does this imply they are purely structural
462 in nature, or do they reflect intrinsic, flexible neural dynamics that transcend task
463 engagement? To advance our understanding of this topic, future research should integrate
464 experience sampling methods with neuroimaging clustering approaches. This combined
465 strategy would allow us to assess whether fluctuations in brain connectivity correspond to
466 variations in conscious experience, shedding light on the functional significance of these
467 brain states and their role in shaping cognition and awareness.

468 Our findings also align with in-silico theoretical models^{47,48}. From a neural dynamics
469 perspective, high-entropy states may reflect a system operating in a metastable regime,
470 allowing for flexible transitions between functional connectivity configurations, a
471 characteristic often associated with wakefulness and cognitive engagement^{45,49}. In
472 contrast, low-entropy states may indicate a system trapped in a more rigid, structurally
473 constrained configuration, which is commonly observed in unconscious states such as
474 deep sleep, anesthesia, and DoC. Notably, the presence of transient high-entropy states
475 in DoC patients suggests that residual network flexibility is preserved to some extent,
476 potentially reflecting brief windows of increased neural complexity that could be relevant
477 for recovery⁴⁵. The prevalence of low-entropy states in healthy controls further
478 underscores that entropy alone is not a direct measure of consciousness but rather one
479 aspect of a broader dynamical framework. Future research should explore how
480 interventions targeting neural network dynamics, such as non-invasive brain stimulation
481 or pharmacological modulation, might influence the stability and transition probabilities of
482 these states, with potential implications for prognosis and therapeutic strategies in DoC.

483 **Conclusion**

484 This study highlights a strong relationship between EEG brain state properties and levels
485 of consciousness. High-entropy brain states are predominantly observed in conscious
486 individuals, while low-entropy states are more prevalent in patients with severe DoC. The
487 occurrence probabilities of these brain states offer crucial insights into patient prognosis.
488 Moreover, we have demonstrated that transient, enhanced connectivity states can be
489 reliably detected in real-time, paving the way for novel diagnostic and therapeutic
490 interventions in DoC patients. By leveraging EEG as a non-invasive, bedside tool, our
491 research contributes to the growing field of digital medicine, enabling continuous, real-
492 time monitoring of brain function. This approach not only deepens our understanding of
493 the neural mechanisms underlying consciousness but also holds the potential to
494 revolutionize clinical workflows with advanced, data-driven diagnostic tools that could
495 transform the care of DoC patients.

496 **Methods**

497 **Ethics statement**

498 All data collections have been approved by their respective ethical committees. The
499 Shanghai study was approved by the Ethical Committee of the Huashan Hospital of Fudan
500 University (approval number: HIRB-2014-281). The Paris study was approved by the
501 Ethical Committee of the Pitié Salpêtrière under the French label of '*Recherche en soins*
502 *courants*' [routine care research]. The Toulouse study was approved by the ethics
503 committee of the University Hospital of Toulouse, Toulouse, France (approval number:
504 RC 31/20/0441). All data collections and analyses were carried out in accordance with the
505 Declaration of Helsinki.

506 **Participants, Recordings and Preprocessing**

507 EEG data were collected from a total of 237 patients and 101 control subjects across three
508 independent datasets (Shanghai, Paris, and Toulouse), resulting in 267 patient recordings
509 and 101 control recordings (see Table S1 for the demographic information). The Shanghai
510 and Paris datasets included chronic patients diagnosed with Minimally Conscious State
511 (MCS) or Unresponsive Wakefulness Syndrome (UWS), while the Toulouse dataset
512 focused on acute patients (see Table S3 for a description of datasets). EEG signals were
513 recorded using Electrical Geodesics systems with high-density electrode nets (HCGSN
514 257-channel for Shanghai and 128-channel for Paris and Toulouse). Sampling rates

515 varied across datasets (1000 Hz in Shanghai, 250 Hz in Paris and Toulouse); therefore,
516 the Shanghai data were downsampled to 250 Hz for consistency. Additionally, all datasets
517 were band-pass filtered between 1–40 Hz to ensure spectral uniformity. To facilitate cross-
518 center comparisons, we interpolated the Shanghai and Paris datasets to match a common
519 128-channel electrode configuration using spherical interpolation (*see Supplementary*
520 *Methods for details*). Preprocessing pipelines followed standard artifact rejection
521 procedures. Clinical assessments were performed using the Coma Recovery Scale-
522 Revised (CRS-R), and only EEG recordings from patients off sedation for at least 24 hours
523 were included.

524 **Dynamic wSMI calculation**

525 wSMI was used to assess non-random joint fluctuations between EEG signals across
526 electrode pairs. A detailed description of the procedure is provided in the Supplementary
527 Methods. Briefly, EEG signals were transformed into symbolic representations using
528 ordinal patterns with an embedding dimension of $d = 3$ (resulting in six possible symbols)
529 and a temporal separation of $\tau = 8$ ms, optimizing sensitivity to a broad frequency range.
530 Mutual information was computed using a modified approach that accounts for symbol
531 similarity, reducing spurious correlations from common EEG sources. *A Current Source*
532 *Density transformation (spherical spline surface Laplacian) was applied before computing*
533 *wSMI*. To capture temporal dynamics, EEG sessions were segmented into overlapping
534 16-second windows with a 1-second shift, balancing sensitivity to brain state transitions
535 while maintaining robust statistical estimation. Connectivity matrices (128×128) were
536 derived for each window and subject. The number of windows varied across datasets due
537 to differences in recording durations, ranging from approximately 8 minutes per subject in
538 the Shanghai dataset to 31 minutes in the Toulouse dataset. All analyses were
539 implemented in Python using NICE Tools, MNE, and scikit-learn⁵⁰.

540 **Unsupervised clustering of connectivity matrices**

541 We applied k -means clustering to identify recurring connectivity patterns, a method widely
542 used in fMRI research^{13,37}. To optimize computational efficiency and ensure equal
543 representation of all EEG recordings, we downsampled each subject's data to 300
544 windows, distributing selections evenly across the session to avoid temporal biases (*see*
545 *Supplementary Methods*). For clustering, we used the Manhattan distance as the similarity
546 metric and determined the optimal number of clusters ($k = 5$) using the Elbow method (Fig.

547 S2). To account for the deterministic nature of *k*-means, we performed 10,000 replicates
548 with randomized centroid initialization to prevent convergence to local minima. Once the
549 centroids were established, all original connectivity matrices were assigned to the closest
550 brain state based on Manhattan distance. Additionally, we computed topographical plots
551 for each centroid by averaging column values across rows in the centroid matrices to
552 obtain a single value per electrode. This analysis was conducted on two datasets: one
553 including all participants (brain states 1–5) and another including only chronic patients
554 (patient-specific brain states PBS1–PBS5), resulting in two distinct sets of brain states.

555 **Brain state complexity and distribution across DoC**

556 The brain states obtained by *k*-means clustering were sorted in descending order based
557 on their entropy. To achieve this, we calculated the entropy of the distribution of wSML
558 values for each centroid by dividing the values into \sqrt{N} bins where $N = 128 \cdot (128 - 1) / 2$ is
559 the number of independent values of the matrix. Additionally, we calculated the Lempel-
560 Ziv complexity (LZC) for each centroid, which quantifies the irreducible information present
561 in a sequence (see Supplementary material for details). The probability of occurrence for
562 each brain state was estimated by determining the proportion of times each individual
563 connectivity matrix was classified as belonging to that specific brain state. This probability
564 was estimated based on all available recording windows, not just the 300 windows
565 selected for clustering.

566 To quantify the shift of brain state distributions towards specific brain states, we introduced
567 a weighted entropy (WE) defined as follows:

$$568 \quad WE = \sum_{i=1}^5 p_i H_i \quad (1)$$

569 Where p_i is the probability of each brain state and H_i is its entropy.

570 Instead of relying solely on the probability distribution of *k*-means centroids, we calculated
571 the entropy of each centroid's connectivity values, which reflects the variability within each
572 pattern. This approach recognizes that even if different centroids have the same
573 probability, their varying entropies will result in different combinations or averages,
574 capturing the underlying complexity of brain states more accurately.

575 Instead of relying solely on the probability distribution of *k*-means centroids, we calculated
576 the entropy of each centroid's connectivity values, reflecting the variability within each

577 pattern. This approach accounts for the fact that some centroids represent more
578 homogeneous and stable connectivity states (lower entropy), while others capture more
579 heterogeneous or rich configurations (higher entropy). si consideramos solo la
580 probabilidad de cada uno de ellos no tendríamos en cuenta esta mayor o menor entropía.
581 Additionally, WE offers a more robust means of comparison across groups, as it ensures
582 that differences in brain dynamics are not solely attributed to frequency shifts but also to
583 changes in the underlying informational structure.

584

585 **Patients' Outcome**

586 We conducted an analysis of the patients' evolution to examine how brain states might
587 provide information regarding their prognosis. For chronic patients, we defined the
588 potential outcomes as improvement in their clinical condition (e.g., UWS patients
589 transitioning to MCS), deterioration (e.g., patients dying or transitioning from MCS to
590 UWS), or no change in their clinical condition. Similarly, for acute patients, the outcomes
591 were determined based on their progression from an acute condition to a chronic
592 condition, including evolution to MCS, evolution to UWS, or death. A summary of the
593 outcomes since recording can be found in Table S1. Patients for whom the outcome was
594 unknown were denoted as "N/A", and their data were excluded from the prognosis
595 analysis.

596 **Real-time simulation**

597 As a proof of concept, we conducted a real-time simulation to assess the feasibility of EEG
598 brain state classification in acute patients. EEG segments were processed at regular
599 intervals, and their functional connectivity patterns were compared to pre-defined offline
600 brain states. We evaluated the consistency between real-time and offline classifications,
601 confirming that the real-time approach reliably captured brain state distributions. These
602 findings support the potential for bedside, real-time monitoring of brain states in disorders
603 of consciousness. Full methodological details are provided in the Supplementary
604 Materials.

605 **Statistical analysis**

606 Group differences were assessed using mixed linear models to evaluate the relationship
607 between WE and levels of consciousness across different patient groups. Specifically, WE
608 was modeled as a function of group category (Healthy, MCS, UWS, and Acute), with
609 dataset center (Shanghai, Paris, and Toulouse) included as a random effect. Multiple
610 comparison corrections were applied to account for differences across conditions,
611 ensuring statistical robustness. In addition, a separate ANOVA was conducted to assess
612 differences within each dataset, followed by post-hoc Tukey HSD tests to determine
613 pairwise significance.

614 To examine the prognostic value of EEG brain states, we analyzed the relationship
615 between WE and patient outcomes in both chronic and acute groups. For chronic patients,
616 a mixed linear model was used to assess whether WE varied across patients who
617 improved, remained stable, or deteriorated. For acute patients, where data were available
618 only from a single center, we performed an ANOVA to compare outcome groups. These
619 analyses allowed us to determine whether specific EEG connectivity patterns were
620 predictive of recovery trajectories in disorders of consciousness.

621 To validate the real-time classification approach, we compared real-time and offline brain
622 state distributions using a bootstrap method and Jensen-Shannon distance analysis. This
623 approach quantified the divergence between the two classification methods, ensuring that
624 real-time EEG monitoring reliably captured the same brain state probabilities as offline
625 analyses. We repeated this comparison across multiple random groupings of patients,
626 demonstrating the robustness of the real-time approach. Full statistical details, model
627 specifications, and additional validation steps are provided in the Supplementary
628 Materials.

629 **Data availability**

630 The data that support the findings of this study are not openly available due to reasons of
631 sensitivity and are available from the corresponding author upon reasonable request.

632 **Code availability**

633 All data was processed using custom MatLab, R and Python software, using specific
634 libraries. Codes are available at <https://github.com/dellabellagabriel/doc-brain-states>.

635 **Acknowledgments**

636 This research was supported by Agencia Nacional de Promoción Científica y Tecnológica,
637 Argentina (Grants #2018-03614, CAT-I-00083) and Stic Amsud project (CONN-COMA,
638 2023). GDB and PB were supported by the National Scientific and Technical Research
639 Council (CONICET - Argentina). DZ was supported by Beijing Natural Science Foundation
640 (7254417) and by National High Level Hospital Clinical Research Funding. PG was
641 supported by the National Natural Science Foundation of China (82201352) and the Youth
642 Innovation Promotion Association of Chinese Academy of Sciences (2022267). LW was
643 supported by the CAS Project for Young Scientists in Basic Research (YSBR-071) and
644 the Shanghai Municipal Science and Technology Major Project (2021SHZDZX). YM and
645 XW were funded by the Shanghai Municipal Science and Technology Major Project
646 ([2018SHZDZX01]), ZJLab and the Shanghai Center for Brain Science and Brain-Inspired
647 Technology. XW was also funded by the National Natural Science Foundation of China
648 (82271224). LW is a SANS (Shanghai Academy of Natural Sciences) Exploration Scholar.

649 We thank Rodrigo Echeveste, Srivas Chennu, Damian Cruse, Demian Engemann,
650 Federico Raimondo and Anat Arzi for useful discussions, and anonymous reviewers for
651 useful suggestions.

652 **Contributions**

653 GADB conceived the project, conceived the analyses, coded and run the analysis,
654 discussed results, wrote the manuscript; DZ conceived the project, designed the
655 experiments and collected the data, conceived the analyses, discussed results, wrote the
656 manuscript; PG conceived the project, designed the experiments and collected the data,
657 conceived the analyses, discussed results, wrote the manuscript; DMM supervised data
658 analysis, wrote the manuscript; JDS, provided data, discussed results, wrote the
659 manuscript; TAB, discussed project and results, wrote the manuscript; DM, collected and
660 provided, wrote the manuscript; BS, collected and provided, wrote the manuscript; FF,
661 collected and provided data, wrote the manuscript; SS, conceived the project, provided
662 data, discussed results, wrote the manuscript; PWL contributed to the implementation of
663 the research, discussed analysis and results, wrote the manuscript; XW contributed to the
664 implementation of the research, wrote the manuscript; YM contributed to the

665 implementation of the research, wrote the manuscript; LW conceived the project,
666 conceived the analyses, discussed data analysis and results; wrote the manuscript; PB
667 conceived the project, conceived the analyses, discussed data analysis and results; wrote
668 the manuscript.

669 **Conflicts of Interest**

670 There are no conflicts of interest

671 **Abbreviations**

672 CRS-R = Coma Recovery Scale Revised; DoC = Disorders of Consciousness; GCS =
673 Glasgow Coma Scale; LZC = Lempel Ziv Complexity; MCS = Minimally Conscious State;
674 UWS = Unresponsive Wakefulness Syndrome; wSMI = weighted Symbolic Mutual
675 Information; WE = Weighted Entropy; TBI = Traumatic Brain Injury; SAH = Subarachnoid
676 Hemorrhage

677 **References**

- 678 1. Edlow, B. L., Claassen, J., Schiff, N. D. & Greer, D. M. Recovery from disorders of
679 consciousness: mechanisms, prognosis and emerging therapies. *Nat. Rev. Neurol.* **17**, 135–
680 156 (2021).
- 681 2. Naccache, L. Minimally conscious state or cortically mediated state? *Brain* **141**, 949–960
682 (2018).
- 683 3. Formisano, R., D’Ippolito, M. & Catani, S. Functional locked-in syndrome as recovery phase
684 of vegetative state. *Brain Inj.* **27**, 1332–1332 (2013).
- 685 4. Laureys, S., Owen, A. M. & Schiff, N. D. Brain function in coma, vegetative state, and related
686 disorders. *Lancet Neurol.* **3**, 537–546 (2004).
- 687 5. Majerus, S., Bruno, M.-A., Schnakers, C., Giacino, J. T. & Laureys, S. The problem of aphasia
688 in the assessment of consciousness in brain-damaged patients. *Prog. Brain Res.* **177**, 49–61
689 (2009).

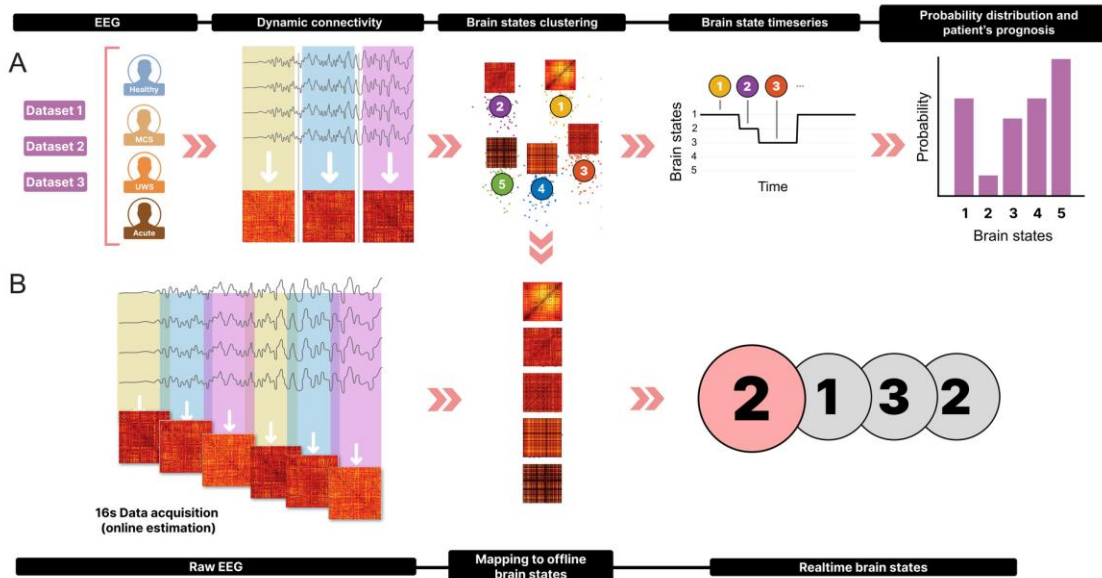
- 690 6. Pincherle, A. *et al.* Early discrimination of cognitive motor dissociation from disorders of
691 consciousness: pitfalls and clues. *J. Neurol.* **268**, 178–188 (2021).
- 692 7. Schnakers, C. *et al.* Diagnostic accuracy of the vegetative and minimally conscious state:
693 Clinical consensus versus standardized neurobehavioral assessment. *BMC Neurol.* **9**, 35
694 (2009).
- 695 8. Casali, A. G. *et al.* A Theoretically Based Index of Consciousness Independent of Sensory
696 Processing and Behavior. *Sci. Transl. Med.* **5**, 198ra105-198ra105 (2013).
- 697 9. Sitt, J. D. *et al.* Large scale screening of neural signatures of consciousness in patients in a
698 vegetative or minimally conscious state. *Brain* **137**, 2258–2270 (2014).
- 699 10. Tagliazucchi, E., Behrens, M. & Laufs, H. Sleep Neuroimaging and Models of Consciousness.
700 *Front. Psychol.* **4**, (2013).
- 701 11. Tononi, G., Sporns, O. & Edelman, G. M. A measure for brain complexity: relating functional
702 segregation and integration in the nervous system. *Proc. Natl. Acad. Sci.* **91**, 5033–5037
703 (1994).
- 704 12. Carhart-Harris, R. *et al.* The entropic brain: a theory of conscious states informed by
705 neuroimaging research with psychedelic drugs. *Front. Hum. Neurosci.* **8**, (2014).
- 706 13. Demertzi, A. *et al.* Human consciousness is supported by dynamic complex patterns of brain
707 signal coordination. *Sci. Adv.* **5**, eaat7603 (2019).
- 708 14. Boly, M. *et al.* Brain connectivity in disorders of consciousness. *Brain Connect.* **2**, 1–10
709 (2012).
- 710 15. Perez Velazquez, J. L., Mateos, D. M., Guevara, R. & Wennberg, R. Unifying biophysical
711 consciousness theories with MaxCon: maximizing configurations of brain connectivity.
712 *Front. Syst. Neurosci.* **18**, (2024).
- 713 16. Mateos, D. M., Erra, R. G., Wennberg, R. & Velazquez, J. L. P. Measures of Entropy and

- 714 Complexity in altered states of consciousness. Preprint at
715 <https://doi.org/10.48550/arXiv.1701.07061> (2017).
- 716 17. Guevara Erra, R., Mateos, D. M., Wennberg, R. & Perez Velazquez, J. L. Statistical mechanics
717 of consciousness: Maximization of information content of network is associated with
718 conscious awareness. *Phys. Rev. E* **94**, 052402 (2016).
- 719 18. Perl, Y. S. *et al.* Non-equilibrium brain dynamics as a signature of consciousness. *Phys. Rev. E*
720 **104**, 014411 (2021).
- 721 19. Miskovic, V., MacDonald, K. J., Rhodes, L. J. & Cote, K. A. Changes in EEG multiscale entropy
722 and power-law frequency scaling during the human sleep cycle. *Hum. Brain Mapp.* **40**, 538–
723 551 (2019).
- 724 20. Olofsen, E., Sleight, J. W. & Dahan, A. Permutation entropy of the electroencephalogram: a
725 measure of anaesthetic drug effect. *Br. J. Anaesth.* **101**, 810–821 (2008).
- 726 21. King, J.-R. *et al.* Information Sharing in the Brain Indexes Consciousness in
727 Noncommunicative Patients. *Curr. Biol.* **23**, 1914–1919 (2013).
- 728 22. Friston, K. J., Stephan, K. E., Montague, R. & Dolan, R. J. Computational psychiatry: the brain
729 as a phantastic organ. *Lancet Psychiatry* **1**, 148–158 (2014).
- 730 23. Dehaene, S., Lau, H. & Kouider, S. What is consciousness, and could machines have it?
731 *Science* **358**, 486–492 (2017).
- 732 24. Dehaene, S. & Changeux, J.-P. Experimental and Theoretical Approaches to Conscious
733 Processing. *Neuron* **70**, 200–227 (2011).
- 734 25. Mashour, G. A., Roelfsema, P., Changeux, J.-P. & Dehaene, S. Conscious Processing and the
735 Global Neuronal Workspace Hypothesis. *Neuron* **105**, 776–798 (2020).
- 736 26. Tononi, G., Boly, M., Massimini, M. & Koch, C. Integrated information theory: from
737 consciousness to its physical substrate. *Nat. Rev. Neurosci.* **17**, 450–461 (2016).

- 738 27. Bekinschtein, T. A. *et al.* Neural signature of the conscious processing of auditory
739 regularities. *Proc. Natl. Acad. Sci.* **106**, 1672–1677 (2009).
- 740 28. Faugeras, F. *et al.* Probing consciousness with event-related potentials in the vegetative
741 state. *Neurology* **77**, 264–268 (2011).
- 742 29. Owen, A. M. *et al.* Detecting awareness in the vegetative state. *Science* **313**, 1402 (2006).
- 743 30. Demertzi, A. *et al.* Intrinsic functional connectivity differentiates minimally conscious from
744 unresponsive patients. *Brain J. Neurol.* **138**, 2619–2631 (2015).
- 745 31. Malagurski, B. *et al.* Topological disintegration of resting state functional connectomes in
746 coma. *NeuroImage* **195**, 354–361 (2019).
- 747 32. Silva, S. *et al.* Disruption of posteromedial large-scale neural communication predicts
748 recovery from coma. *Neurology* **85**, 2036–2044 (2015).
- 749 33. Massimini, M. Breakdown of Cortical Effective Connectivity During Sleep. *Science* **309**,
750 2228–2232 (2005).
- 751 34. Stender, J. *et al.* Diagnostic precision of PET imaging and functional MRI in disorders of
752 consciousness: a clinical validation study. *Lancet Lond. Engl.* **384**, 514–522 (2014).
- 753 35. Ferrarelli, F. *et al.* Breakdown in cortical effective connectivity during midazolam-induced
754 loss of consciousness. *Proc. Natl. Acad. Sci.* **107**, 2681–2686 (2010).
- 755 36. Rosanova, M. *et al.* Recovery of cortical effective connectivity and recovery of
756 consciousness in vegetative patients. *Brain J. Neurol.* **135**, 1308–1320 (2012).
- 757 37. Allen, E. A. *et al.* Tracking Whole-Brain Connectivity Dynamics in the Resting State. *Cereb.*
758 *Cortex N. Y. NY* **24**, 663–676 (2014).
- 759 38. Barttfeld, P. *et al.* Signature of consciousness in the dynamics of resting-state brain activity.
760 *Proc. Natl. Acad. Sci.* **112**, 887–892 (2015).
- 761 39. Tasserie, J. *et al.* Deep brain stimulation of the thalamus restores signatures of

- 762 consciousness in a nonhuman primate model. *Sci. Adv.* **8**, eabl5547 (2022).
- 763 40. Deco, G. *et al.* Awakening: Predicting external stimulation to force transitions between
764 different brain states. *Proc. Natl. Acad. Sci.* **116**, 18088–18097 (2019).
- 765 41. Kringelbach, M. L. & Deco, G. Brain States and Transitions: Insights from Computational
766 Neuroscience. *Cell Rep.* **32**, 108128 (2020).
- 767 42. Kodinariya, T. & Makwana, P. Review on Determining of Cluster in K-means Clustering. *Int. J.*
768 *Adv. Res. Comput. Sci. Manag. Stud.* **1**, 90–95 (2013).
- 769 43. Uhrig, L. *et al.* Resting-state Dynamics as a Cortical Signature of Anesthesia in Monkeys.
770 *Anesthesiology* **129**, 942–958 (2018).
- 771 44. Giacino, J. T., Fins, J. J., Laureys, S. & Schiff, N. D. Disorders of consciousness after acquired
772 brain injury: the state of the science. *Nat. Rev. Neurol.* **10**, 99–114 (2014).
- 773 45. Sanz Perl, Y. *et al.* Perturbations in dynamical models of whole-brain activity dissociate
774 between the level and stability of consciousness. *PLOS Comput. Biol.* **17**, e1009139 (2021).
- 775 46. Luppi, A. I. *et al.* Consciousness-specific dynamic interactions of brain integration and
776 functional diversity. *Nat. Commun.* **10**, 4616 (2019).
- 777 47. Deco, G., Vidaurre, D. & Kringelbach, M. L. Revisiting the global workspace orchestrating the
778 hierarchical organization of the human brain. *Nat. Hum. Behav.* **5**, 497–511 (2021).
- 779 48. Kringelbach, M. L. *et al.* Dynamic coupling of whole-brain neuronal and neurotransmitter
780 systems. *Proc. Natl. Acad. Sci.* **117**, 9566–9576 (2020).
- 781 49. Tagliazucchi, E. & Laufs, H. Decoding Wakefulness Levels from Typical fMRI Resting-State
782 Data Reveals Reliable Drifts between Wakefulness and Sleep. *Neuron* **82**, 695–708 (2014).
- 783 50. Pedregosa, F. *et al.* Scikit-learn: Machine Learning in Python. *J Mach Learn Res* **12**, 2825–
784 2830 (2011).

785 **Figures and Tables**

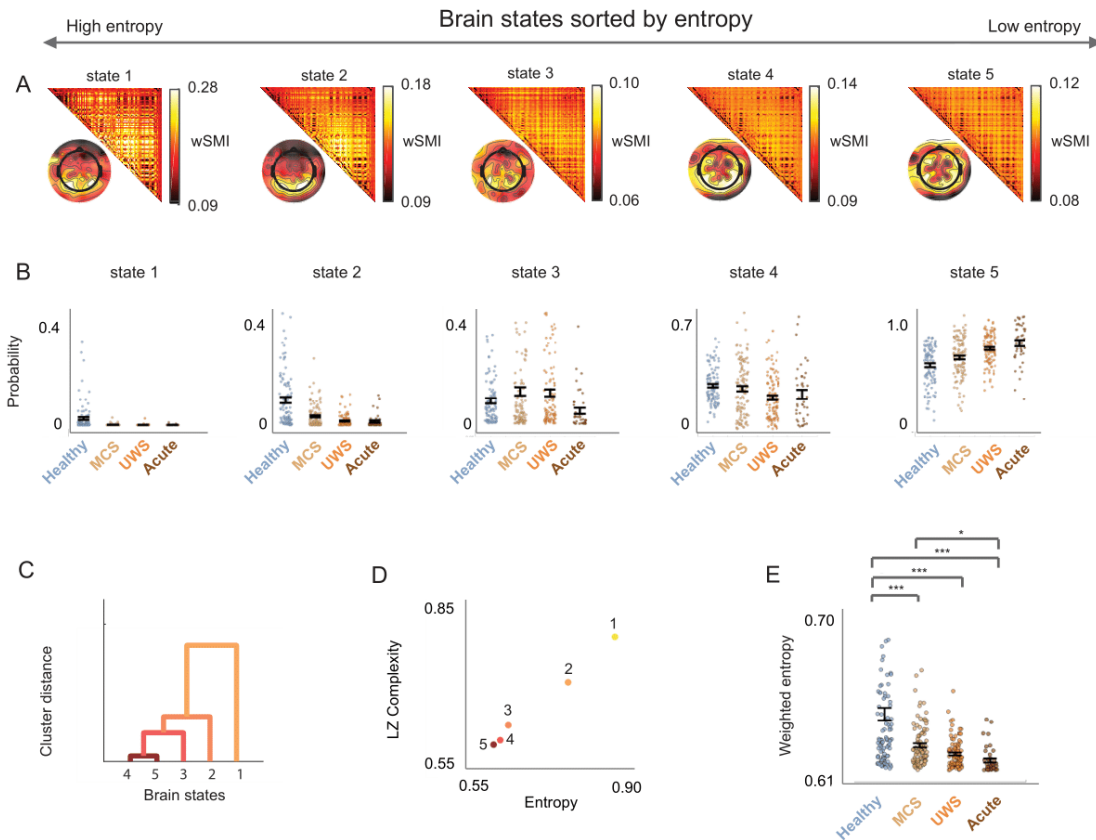


786

787 **Figure 1. Analysis pipeline.** A) Offline calculation of brain states: We utilized three
 788 datasets from different centers, comprising healthy controls and three patient categories
 789 (Minimally Conscious Syndrome [MCS], Unresponsive Wakefulness Syndrome[UWS],
 790 and Acute patients). Windowed wSMI matrices were computed from EEG data, followed
 791 by clustering analysis to identify 5 distinct brain states. The probability and association
 792 with patient prognosis were then evaluated. B) Real-time calculation of brain states:
 793 Simulating a bedside scenario, we processed 16 seconds of raw EEG data every 24
 794 seconds to generate raw-data wSMI matrices. By matching these matrices to the pre-
 795 defined brain states obtained offline, we established real-time brain state identification.

796

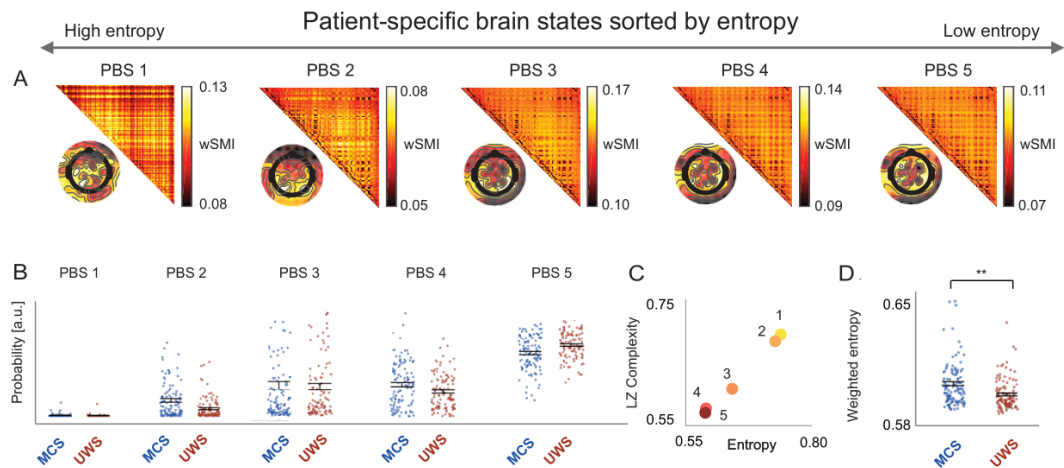
797



798

799 **Figure 2. EEG brain states and their distribution in DoC.** A) Brain states ordered by
 800 entropy from 1 (high entropy) to 5 (low entropy). The upper triangular part of the matrices
 801 represents the centroids, or brain states, obtained from the clustering analysis. The value
 802 at row i and column j indicates the wSMI connectivity between electrode i and electrode j .
 803 The topographical plots illustrate the average of wSMI values for each electrode. B)
 804 Probability distributions of brain states across all groups. Brain state 1 is predominantly
 805 observed in healthy subjects, whereas the probability of brain state 5 increases with the
 806 severity of DoC. C) Dendrogram clustering displaying the Manhattan distances between
 807 brain states. D) Lempel-Ziv complexity as a function of entropy for each brain state. Brain
 808 States with higher variance exhibit greater entropy and Lempel-Ziv complexity. E)
 809 Weighted entropy across all groups, highlighting changes in entropy as a function of DoC
 810 severity (p -values corrected for multiple comparisons. * $p < 0.05$, *** $p < 0.001$).

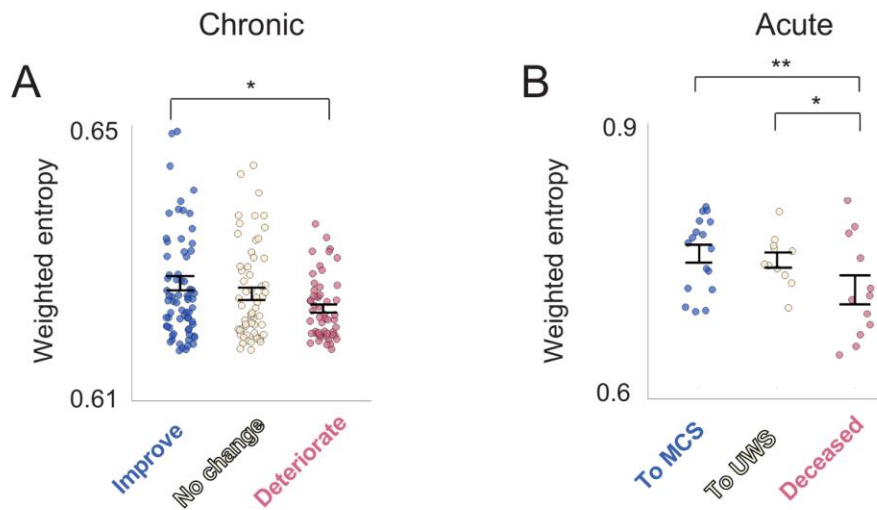
811



812

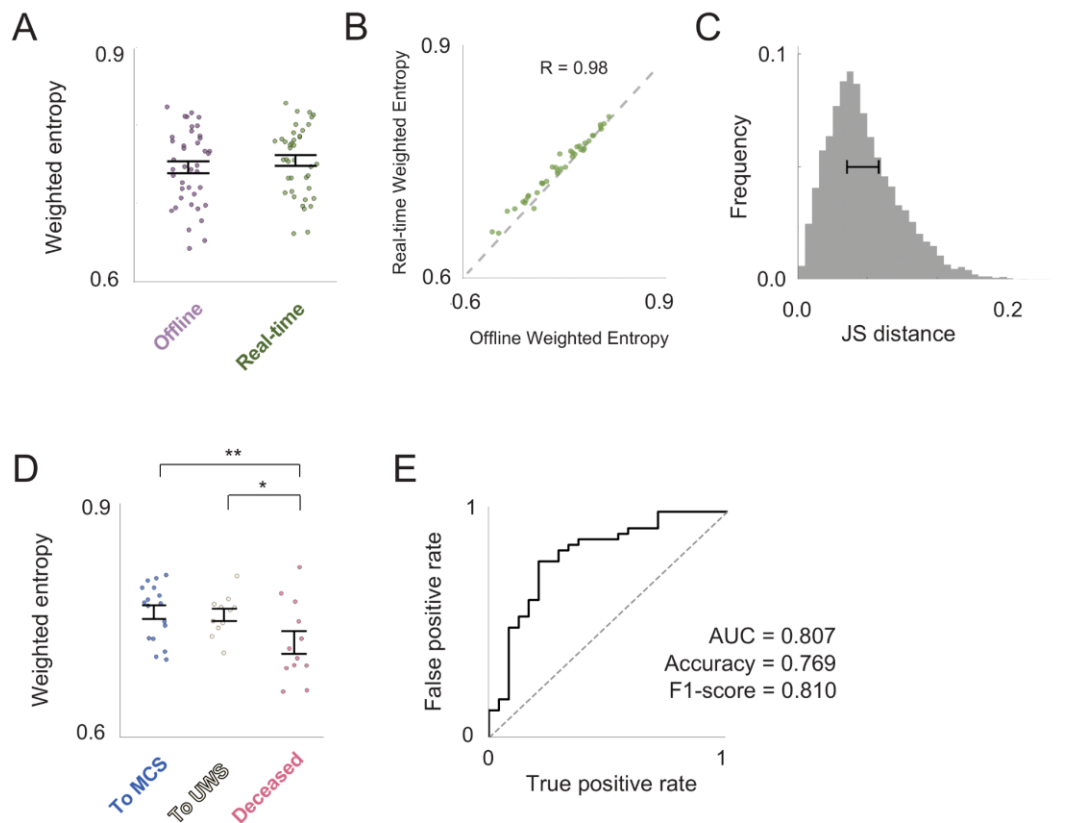
813 **Figure 3. Patient-specific brain states.** A) Brain states defined using data exclusively
 814 from chronic patients. The upper triangular part of the matrices correspond to the
 815 centroids, a.k.a brain states resulting from the clustering analysis, and the value at row i
 816 and column j represents the wSMI connectivity value between electrode i and electrode j
 817 with brain states sorted by entropy from 1 (high entropy) to 5 (low entropy). The
 818 topographical plots show the average wSMI value for each electrode. B) Probability
 819 distribution of all 5 brain states for MCS and UWS. C) Lempel-Ziv complexity as a function
 820 of entropy for each patient-specific brain state. D) WE for both groups. The weighted
 821 entropy values follow the same trend, supporting the differentiation of brain states based
 822 on the level of consciousness. (p-values were corrected for multiple comparisons, $**p <$
 823 0.01).

824



825

826 **Figure 4. Relationship between brain states and patients' prognosis.** A) WE as a
 827 function of chronic patients' outcome. The graph shows that in chronic patients, the WE
 828 tends to be higher as the probability of patient improvement increases. B) WE as a function
 829 of acute patients' outcomes. Similarly, in acute patients, the WE tends to be higher in
 830 patients who show improvement in their condition. (p-values were corrected for multiple
 831 comparisons, *p < 0.05, **p < 0.01).

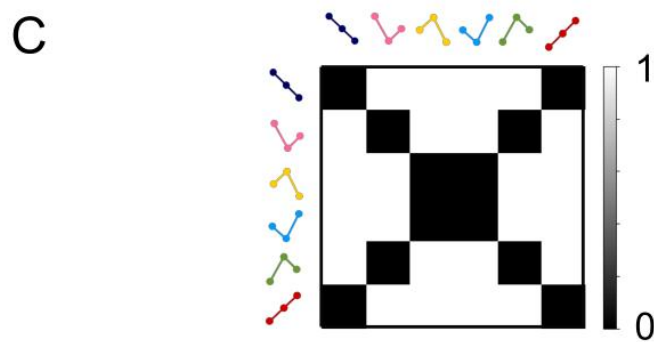
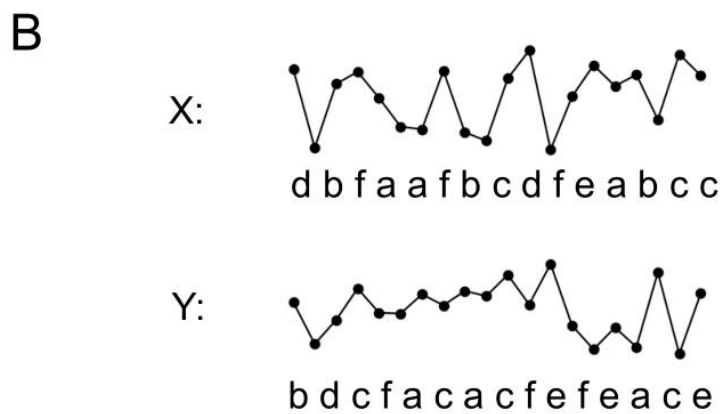
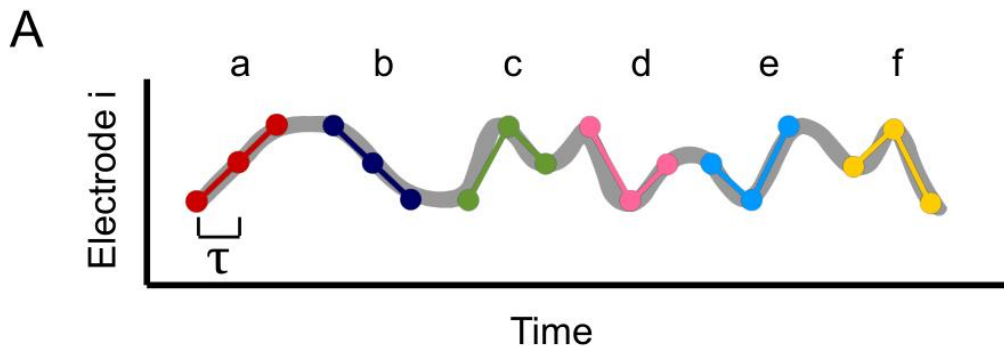


832

833 **Figure 5. Real-time EEG brain states.** A) WE values calculated for acute patients, using
 834 both offline and real-time methods. B) Individual WE values calculated in real-time closely
 835 matched those obtained through the offline procedure, which included EEG signal
 836 cleaning and proper preprocessing. C) The null distribution of Jensen-Shannon distance
 837 values between random partitions of the offline data is shown. The error bar represents
 838 the estimated value and uncertainty for the real-time calculations, which fall within the
 839 distribution, demonstrating the reliability of real-time WE estimation. D) Prognosis as a
 840 function of WE values calculated in real-time. D) Classification of patients versus controls
 841 based on real-time data. (p-values were corrected for multiple comparisons, *p < 0.05, **p
 842 < 0.01).

843

844



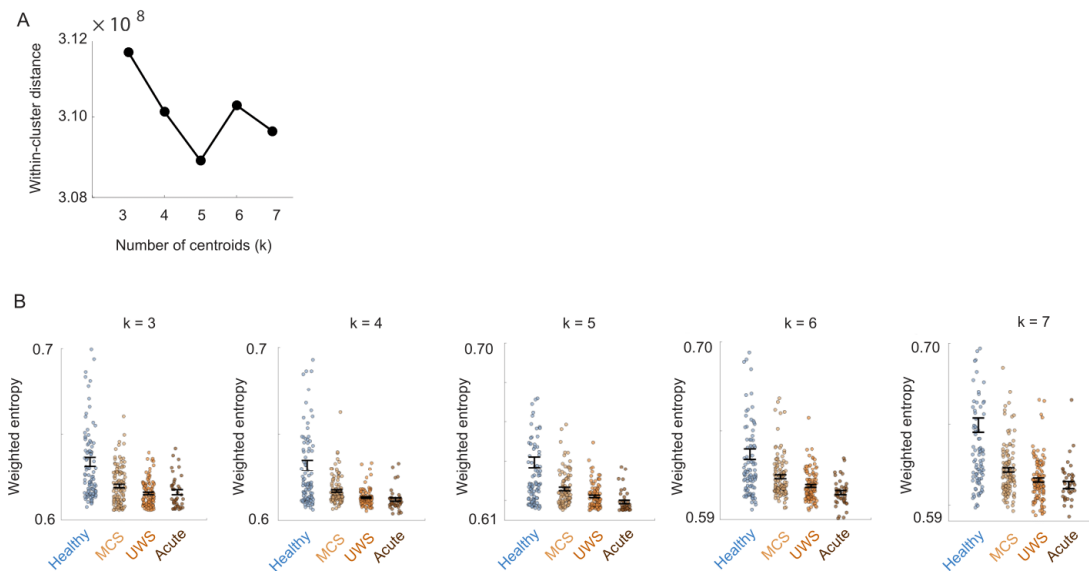
845

846 **Supplementary Figure 1. Schematic of the Weighted Symbolic Mutual Information**

847 **Calculation.** A) The continuous EEG time series from each electrode is transformed into

848 a discrete sequence of symbols. Each symbol consists of three elements, with each

849 sample separated by a time delay (τ), resulting in a total of six possible symbols based on
 850 the signal pattern. B) Once the signal is transformed into its discrete version, a time series
 851 of symbols is obtained for each electrode. This allows for the computation of the joint
 852 probability distribution between electrodes X and Y, enabling the calculation of Symbolic
 853 Mutual Information. C) To prevent contamination from passive cranial conductivity
 854 artifacts, and in accordance with methodological references, the mutual information matrix
 855 is weighted by disregarding equal and opposite symbols. Additionally, diagonal elements,
 856 representing mutual information calculations between identical channels, are removed to
 857 ensure that only non-identical symbols contribute to the final wSMI measure.

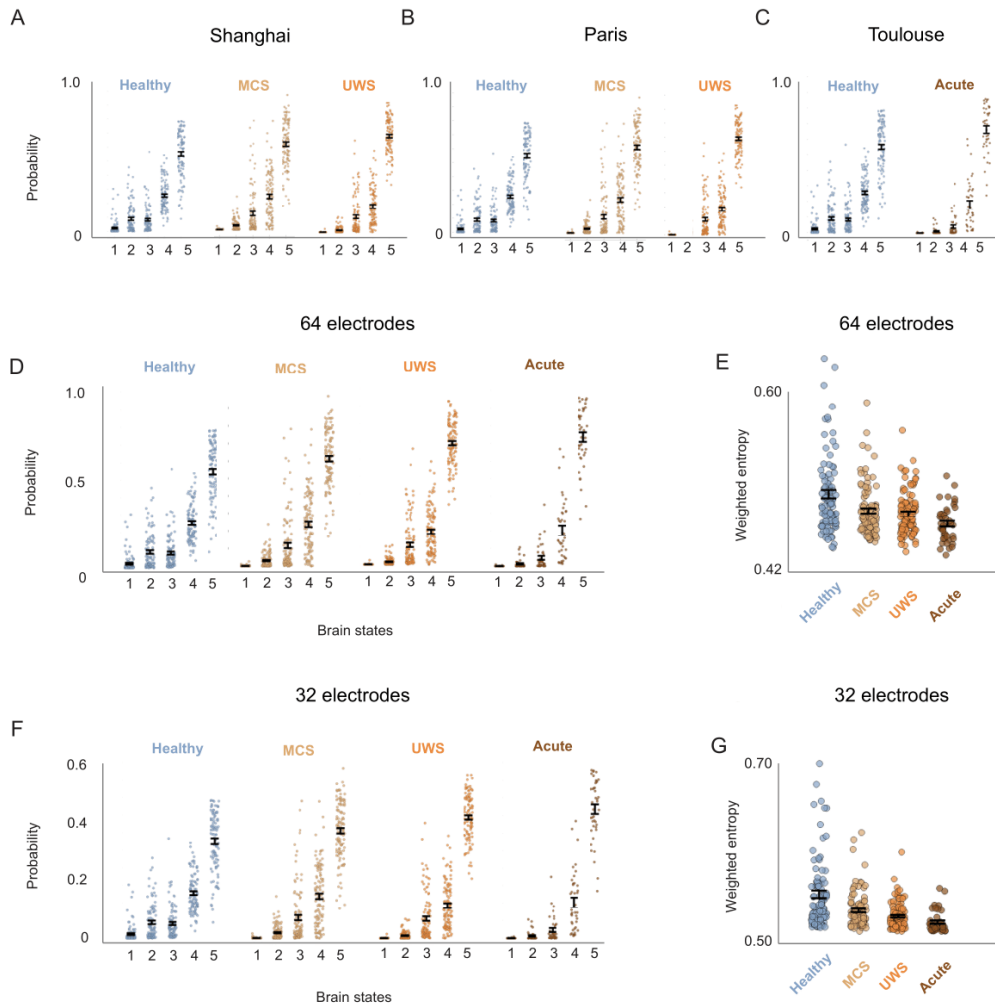


858

859 **Supplementary Figure 2. Optimal Number of Clusters.** A) Within-cluster distance as a
 860 function of the number of clusters (k) for k = 3 to 7. The within-cluster distance reaches its
 861 minimum at k = 5 (the "elbow"), indicating that this is the optimal number of clusters that
 862 balance compactness and interpretability. B) WE across conditions for k = 3 to k = 7.
 863 Regardless of the number of centroids considered, WE decreases monotonically from
 864 Healthy to Acute, demonstrating a robust trend across clustering solutions.

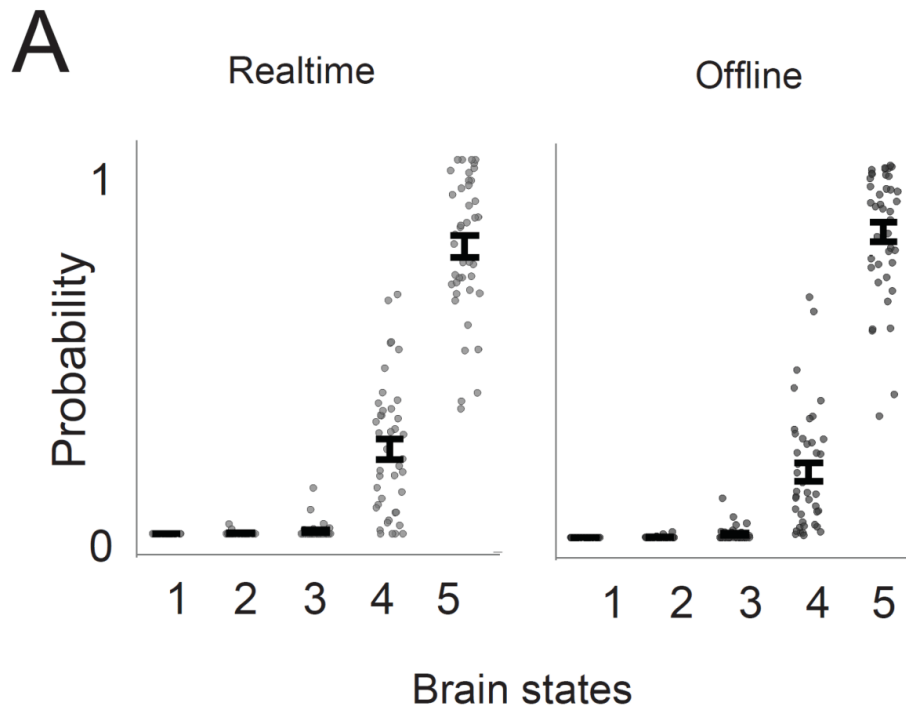
865

874 locations. C) Probability distribution across conditions using brain states obtained from
 875 Shanghai (top), Paris (middle) and Toulouse (bottom).



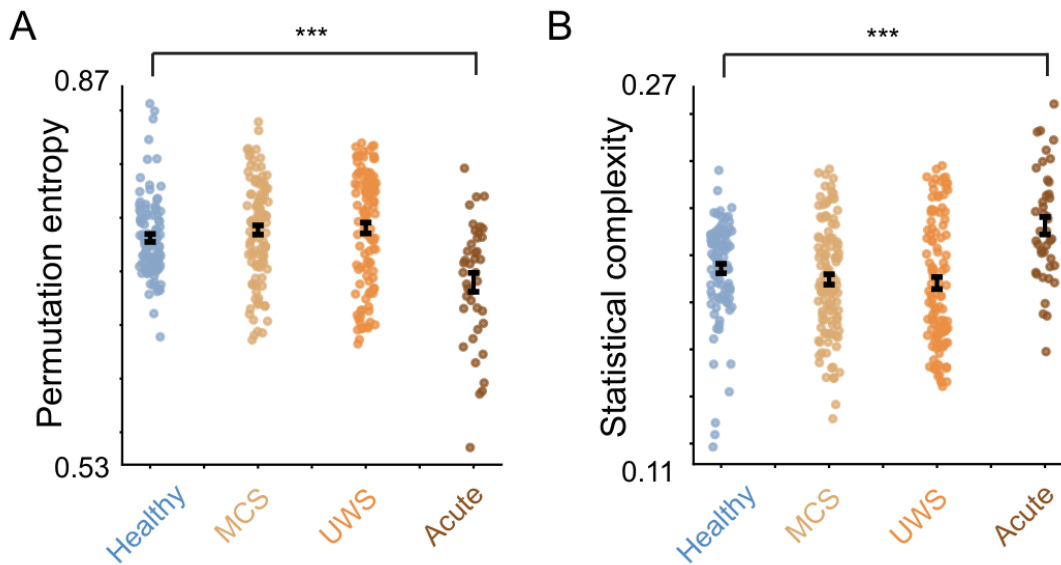
876

877 **Supplementary Figure 4. Consistency of Brain States Across Datasets and**
 878 **Electrode Number.** A-C) Brain states ordered by entropy from 1 (high entropy) to 5 (low
 879 entropy), calculated independently for all centers. The brain states display a consistent
 880 pattern across datasets, with high-entropy states associated with healthy subjects and the
 881 frequency of low-entropy states correlating with the severity of the condition in patients.
 882 D) Probability distribution obtained with 64 electrodes. E) WE obtained with 64 electrodes.
 883 F) Probability distribution obtained with 32 electrodes. G) WE obtained with 32 electrodes.



884

885 **Supplementary Figure 5. Real time and offline acute-patient brain state**
 886 **distributions.** Comparison of brain state distributions in acute patients obtained through
 887 real-time and offline EEG analyses. This figure illustrates the consistency between real-
 888 time estimations and offline calculations, highlighting the reliability of real-time EEG-based
 889 brain state assessments.



890

891 **Supplementary Figure 6. Entropy and Complexity of the Timeseries.** A) Shannon
 892 entropy of the timeseries across conditions. Entropy is lower in Acute compared to the
 893 other conditions, with a statistically significant difference relative to Healthy (** $p < 0.001$).
 894 B) Statistical complexity of the timeseries for each condition. Complexity is higher in Acute
 895 compared to the other conditions, with a statistically significant difference relative to
 896 Healthy (** $p < 0.001$).

897 **Supplementary Table 1. Age and gender for all participants.**

898 **Supplementary Table 2. Correlation between brain states obtained from different**
 899 **experimental conditions.** Participants listened to words, phrases and sentences while
 900 EEG was recorded.

901 **Supplementary Table 3. Summary of preprocessing parameters for the three sites.**